On Increasing the Accuracy of Simulations of Deposition and Etching Processes Using Radiosity and the Level Set Method

Clemens Heitzinger and
Siegfried Selberherr
Institute for Microelectronics, TU Wien
Gusshausstrasse 27-29
A-1040 Vienna, Austria
Heitzinger@iue.tuwien.ac.at

Josef Fugger and
Oliver Häberlen
Infineon Technologies
Siemensstrasse 2
A-9500 Villach, Austria
Oliver.Haeberlen@infineon.com

Abstract

Deposition and etching in Silicon trenches is an important step of today's semiconductor manufacturing. Understanding the surface evolution enables to predict the resulting profiles and thus to optimize process parameters. Simulations using the radiosity modeling approach and the level set method provide accurate results, but their speed has to be considered when employing advanced models and for purposes of inverse modeling.

In this paper strategies for increasing the accuracy of deposition simulations while decreasing simulation times are presented. Two algorithms were devised: first, intertwining narrow banding and extending the speed function yields a fast and accurate level set algorithm. Second, an algorithm which coarsens the surface reduces the computational demands of the radiosity method.

Finally measurements of a typical TEOS *deposition process are compared with simulation results both with and without coarsening of the surface elements. It was found that the computational effort is significantly reduced without sacrificing the accuracy of the simulations.*

1. Introduction

Deposition and etching in Silicon trenches are crucial processes in today's semiconductor manufacturing, e.g. for state of the art memory cells and Power MOSFETs. In order to understand and simulate the transport of gas species and the surface evolution, and thus to achieve void-less filling of deep trenches, to predict the resulting profiles, and to optimize process parameters with respect to manufacturing throughput and the quality of the resulting trenches, a general purpose topography simulator was developed based on the level set method and advanced physical models. In the following two strategies for reducing computation time and thus increasing the accuracy of the simulations are presented. They were implemented in the framework of the simulator, which consists of a level set module, a radiosity module, a diffusion module, and a surface reaction module.

In several experiments SiO_2 layers were deposited into trenches roughly $4\mu\mathrm{m}$ deep and $2\mu\mathrm{m}$ wide, where the final layer thickness was in the range of $1\mu\mathrm{m}$ for the flat wafer surface. In order to make the predictions of the simulation more accurate, model parameters were extracted by comparing the step coverages of the deposited layers in the simulation with those of SEM (scanning electron microscope) images.

After describing two methods for reducing the computational effort of these simulations, simulation results are discussed and simulation times compared. The simulations reproduced the shapes of the trenches very well and good quantitative agreement was achieved as well. The effects of the surface coarsening algorithm on the accuracy of the simulations and their computational effort were found to be very satisfactory.

Finally, it is noted that the methods presented allow to achieve the high resolutions which are indispensible for the accurate simulation of the surface evolution at the trench opening, the trench bottom, and also for the effects of microtrenching and side wall push back within workable simulation times.

2. Narrow Banding and Extending the Speed Function

The level set method is based on representing surfaces as the zero level set of a function $u(t, \mathbf{x})$ and solving the partial differential equation $u_t + F(t, \mathbf{x})\|\nabla_{\mathbf{x}} u\| = 0$, $u(0, \mathbf{x})$ given, where $F(t, \mathbf{x})$ is the speed function determining the speed points of the surface move in direction normal to it. The advantages of the level set method are twofold: the resolution achieved is higher than the resolution of the grid where the calculations take place, and hence higher than the resolution achieved using a cellular format on a grid of the same size [1, 2]. Furthermore, calculating surface normals, crucial for radiosity simulations, is more precise than when using a cellular format.

For the first time narrow banding and extending the speed function were combined into one algorithm. This algorithm provides several benefits. First, the speed function is retained as the signed distance function throughout

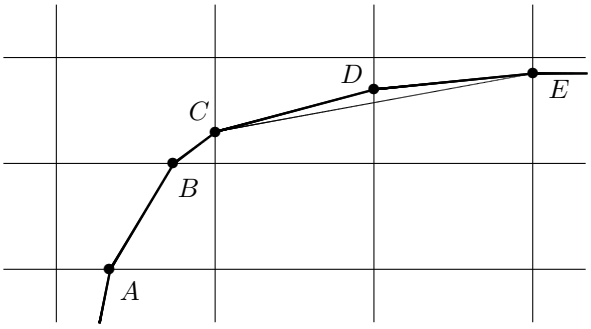

Figure 1. Illustration of the coalescing algorithm. Since the angles at A, B, and C are above the threshold value, no replacement takes place here. The angle at D is below the threshold value, and thus the segments CD and DE are replaced by a new segment CE.

the simulation, which assures good accuracy till the end of the simulation. Second, narrow banding reduces the number of active points that have to be updated from $O(n^2)$ to $O(n)$. By retaining the signed distance function the width of the narrow band is kept down to two points on each side (cf. Figure 4) without decreasing accuracy. Third, time consuming calculations (cf. [3]) are reduced to a minimum by intertwining the computations necessary for narrow banding and extending the speed function. Finally, it is noted that the width of the narrow band can be adjusted if desired.

The algorithm works as follows. First the initial points near the zero level set, where the speed function is known, and the neighboring trial points are determined. In the main loop it is checked if there is still a trial point to be considered in the narrow band. All trial points are stored in a heap ordered by their distance to the zero level set. If there is a point to be considered, both its distance is approximated and its extension speed calculated, and its neighbors are updated accordingly. Finally after the main loop, bookkeeping information for the narrow band points is updated using distance information just computed. The computation time consumed by this algorithm is negligible compared to that required for the physical models, while it provides high accuracy.

3. Coalescing Surface Elements

When using radiosity models for simulating the transport of particles above the wafer in the case where the length of the mean free path is greater than the size of the feature, two operations consume the most part of the computation time. The first operation is determining the visibility between all surface elements, which is an $O(n^2)$ operation, where n denotes the number of surface elements extracted from the level set grid. The second operation is solving a certain system of linear equations, which leads to calculating the inverse of a matrix with n^2 elements, which is an $O(n^3)$ operation.

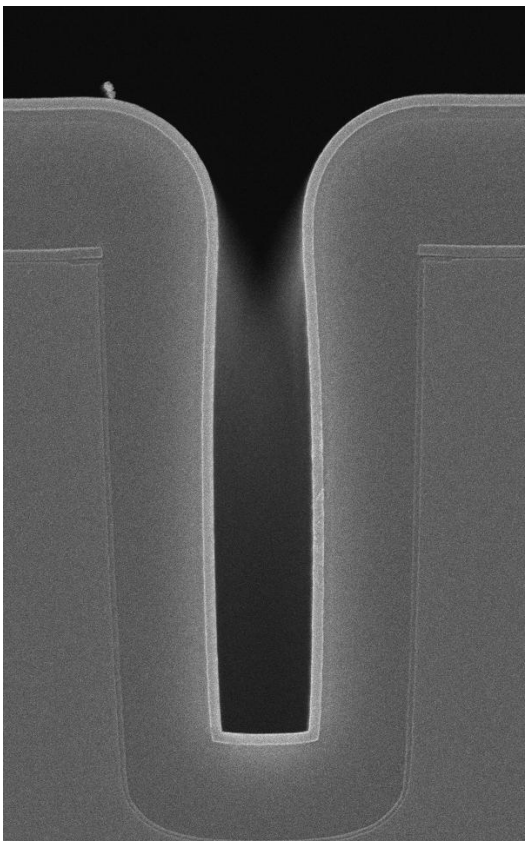

Figure 2. One of the images of a vertical trench for a Power MOSFET approximately $2\,\mu\mathrm{m}$ wide and $4\,\mu\mathrm{m}$ deep.

Obviously increasing the number of surface elements is not a remedy in cases where high resolution is required. High resolution is needed, e.g., near the trench opening, and the bottom of the trench, and for the simulation of microtrenching and side wall push back. One approach is to devise a refinement and coarsening strategy for unstructured grids at the level of the level set implementation and the algorithms working on it. This, however, complicates the fast marching algorithm necessary for extending the speed function. A different approach was taken in this work by coarsening the surfaces after having been extracted from the level set grid.

The algorithm works by walking down the list of surface elements extracted as the zero level set and calculating the angle α between two neighboring surface elements. Whenever $|\pi - \alpha|$ is below a certain threshold value of a few degrees, the neighboring elements are coalesced into one. After one sweep through the list, the algorithm can be reapplied for further coarsening. After k coarsening sweeps, at most 2^k surface elements are coalesced into one. The resulting longer surface elements are used for the radiosity calculation, after which the fluxes are translated back from the coarsened elements to the original ones.

A formulation of the radiosity method for the transport of particles of low energy only, where luminescent reflection is assumed, which excludes the case of high energetic

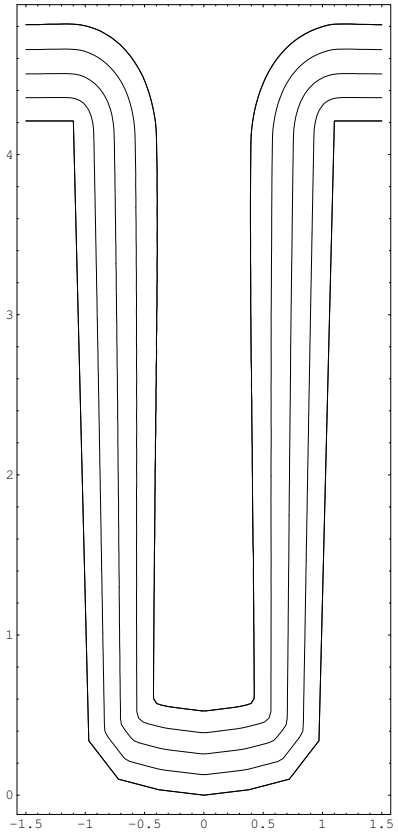

Figure 3. A simulation result showing initial, intermediate, and final surfaces. The resolution of the underlying level set grid was $80 \cdot 160$. The coarsening algorithm was applied twice, coalescing at most four surface elements into one, and the threshold angle was $3°$. This result is nearly identical to the one achieved when no coarsening was applied.

particles, can be found, e.g., in [4]:

$$\text{Flux} = \frac{\beta - \beta_0}{1-\beta} I_S + \\ + \frac{\beta(1-\beta_0)}{1-\beta} \underbrace{L^{-1}(L^{-1} - (1-\beta)\Psi)^{-1}}_{T:=} I_S,$$

where I_S is the vector of fluxes coming from the sources to the surface elements, β_0 the sticking coefficient for particles coming directly from the source, β the one for secondary bounces, L the diagonal matrix containing the lengths of the surface elements, and

$$\Psi_{ij} = \frac{n_i \cdot (t_j - t_i) n_j \cdot (t_i - t_j)}{\pi |t_j - t_i|^3} [i \text{ visible } j],$$

where t_i are the centroids of the surface elements, n_i their unit normal vectors, and $[i$ visible $j]$ is 1 or 0 if surface element j is visible from i respectively not.

We note that in the case of multiple, low energy species the calculation of the visibility matrix and the inverse T only depends on topographic information and thus does not have to be repeated for each species.

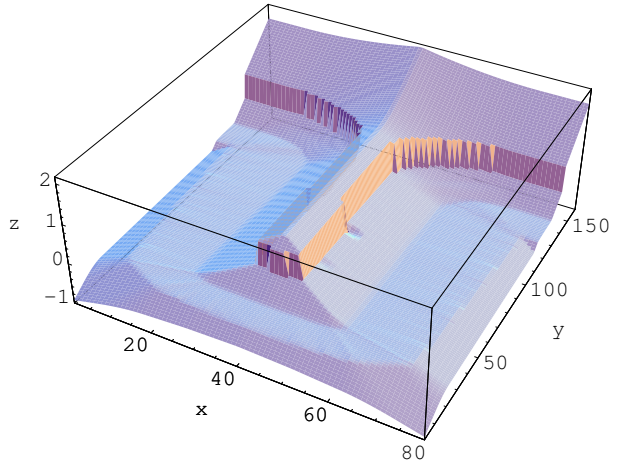

Figure 4. The level set function after the last step of the simulation whose result is shown in Figure 3. The active narrow band around the zero level set retains the signed distance function, whereas other grid points have not been updated.

4. Simulation Results

Before discussing the simulations and the effects of the speeding up strategies, the physical modeling approach is shortly described.

In order to calculate the thickness Δd of the film deposited during a time interval of length Δt, we observe that Δd is proportional to Δt, to an Arrhenius term, and to the deposition rate R_i corresponding to the deposition model chosen. This implies $\Delta d = \Delta t \cdot k_e \mathrm{e}^{-E/kT} \cdot R_i$. Here $k_e \mathrm{e}^{-E/kT}$ is the Arrhenius term with activation energy E, absolute temperature T, and preexponential constant k_e. R_i is the deposition rate of the deposition model chosen, where two heterogeneous deposition models, a homogeneous intermediate-mediated deposition model, and a heterogeneous deposition with byproduct inhibition model are available [5]. This setup also provides a way to determine the actual chemical reaction, which is a nontrivial problem and can only be done indirectly by comparing measurements and simulation results.

Several SEM images of trenches about $4\,\mu\mathrm{m}$ deep and $2\,\mu\mathrm{m}$ wide were used for comparing the step coverages of simulated deposition processes with reality. First, it is noted that the computation time of the level set algorithm with narrow banding as described above (cf. Figures 4, 5, and 6) is negligible compared to the computation time of the physical models. This, however, is not the case when narrow banding is not employed. Table 1 lists the relative computation time of testing for visibility and the actual radiosity calculation both with and without the coalescing algorithm. The simulation result with coarsening in Figure 3 is nearly identical to the one yielded when no coarsening was applied. Accuracy is hardly affected, but the simulation time considerably decreased.

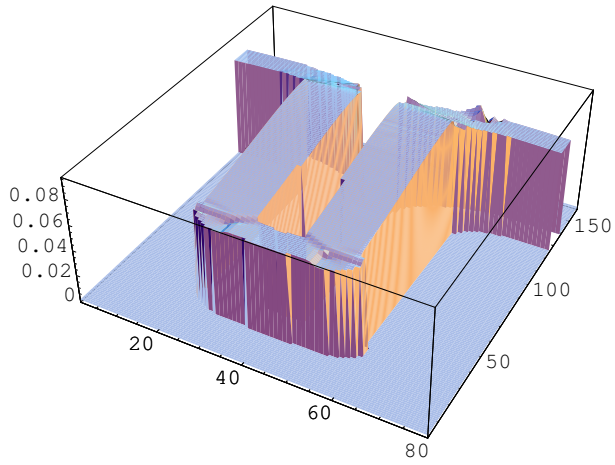

Figure 5. The extended speed function in the narrow band in the last step of a simulation. In this simulation, no coarsening was performed, but apart from that it is identical to the one leading to Figure 3.

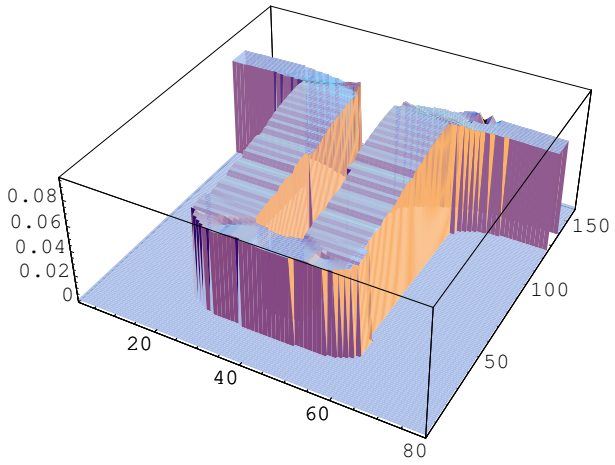

Figure 6. The extended speed function in the narrow band in the last step of the simulation leading to Figure 3. The coarsening can clearly be seen at the side walls of the trench.

Table 1. Comparison of the speed of the visibility test and of the calculation of the fluxes on surface elements by radiosity both with the coalescing algorithm and without. The computation time relative to the conventional algorithm, equaling 1, is shown.

Coarsening Steps	Visibility Test	Flux Calculation
0	1	1
1	0.29	0.10
2	0.12	0.02

5. Conclusion

Two strategies for increasing the accuracy of radiosity simulations are presented and compared to measurements of a deposition process. The first method is an algorithm which performs three level set computations in parallel: calculating the signed distance function via a fast marching algorithm, extending the speed function, and moving the narrow band according to the new zero level set. This gives rise to a fast and accurate level set algorithm.

The second method is a coarsening algorithm which ensures fine resolution of the surface in parts of the boundary with relatively high curvature, i.e., where it is needed most. These parts are typically the opening of the trench, its bottom, and places where microtrenching and side wall push back take place. At the same time the resolution is lowered where possible which reduces the computational demand significantly.

These algorithms were implemented in a general purpose deposition and etching simulator which consists off four independent modules, namely the level set module, a reaction module, a diffusion module, and a radiosity module. It can be used for simulating all common deposition and etching processes.

A TEOS deposition process was simulated by this simulator and its parameters adjusted to measurements. To that end, the step coverages of the measurements were compared to those of the simulations and good quantitative agreement was achieved. Simulations both with and without the surface coalescing algorithm were carried out, which showed that it reduces simulation time for given accuracies in the trade off between accuracy and simulation time.

6. Acknowledgment

The authors acknowledge support from the “Christian Doppler Forschungsgesellschaft,” Vienna, Austria.

[1] W. Pyka, R. Martins, and S. Selberherr, “Optimized Algorithms for Three-Dimensional Cellular Topography Simulation,” *IEEE J.Technology Computer Aided Design*, no. 20, 2000. `http://www.ieee.org/products/online/journal/tcad/accepted/Pyka-March00/`.

[2] A. Hössinger, T. Binder, W. Pyka, and S. Selberherr, “Advanced Hybrid Cellular Based Approach for Three-Dimensional Etching and Deposition Simulation,” in *Simulation of Semiconductor Processes and Devices*, (Athens, Greece), pp. 424–427, Sept. 2001.

[3] D. Adalsteinsson and J. Sethian, “The Fast Construction of Extension Velocities in Level Set Methods,” *J.Comput.Phys.*, vol. 148, no. 1, pp. 2–22, 1999.

[4] J. Sethian, *Level Set Methods and Fast Marching Methods*. Cambridge: Cambridge University Press, 1999.

[5] G. Raupp, F. Shemansky, and T. Cale, “Kinetics and Mechanism of Silicon Dioxide Deposition Through Thermal Pyrolysis of Tetraethoxysilane,” *J.Vac.Sci.Technol.B*, vol. 10, pp. 2422–2430, Nov. 1992.